ELSEVIER

Polymer Vol. 37 No. 1, pp. 11–18, 1996

0032-3861/96/$15.00+0.00

High-resolution solid-state ^{13}C nuclear magnetic resonance study of a polymer complex: poly(methacrylic acid)/ poly(ethylene oxide)

Toshikazu Miyoshi*†, K. Takegoshi† and Kunio Hikichi
Section of Structural Bio-Macromolecular Science, Division of Biological Sciences, Graduate School of Science, Hokkaido University, Sapporo 060, Japan
(Received 21 April 1995; revised 14 June 1995)

The inter-polymer interaction, morphology and molecular motion of the poly(ethylene oxide)/ poly(methacrylic acid) (PEO/PMAA) complex were investigated by measuring various nuclear magnetic resonance parameters, such as ^{13}C chemical shift, $^{1}H\ T_1$, $^{1}H\ T_{1\rho}$, $^{1}H\ T_2$ and $^{13}C\ T_2$. For the complex, we observed two peaks for the carboxyl carbon of PMAA. We assigned the higher-field resonance to the carboxyl group that forms hydrogen bonds to PEO (the complex form), and the lower-field one to the group that forms hydrogen bonds among PMAA (the dimeric form). It is shown that, for temperatures within 100 K below T_g, the complex form easily breaks up and rearranges to the dimeric form. For the complex, the $^{13}C\ T_2$ and $^{1}H\ T_2$ reveal that PEO is mobile, whereas PMAA is rigid. This different mobility between PEO and PMAA may facilitate breakage of the hydrogen bonding between PEO and PMAA. Examination of ^{1}H spin diffusion in the complex reveals that the distance between PEO and PMAA in the complex is similar to that between PEO and PMAA in the dimeric form. These results show that the PMAA in the dimeric form does not aggregate to form a domain structure, and that the PEO/PMAA complex is miscible on a segmental scale. Furthermore, the thermal degradation of PMAA in the complex was examined. Dehydration occurs in the dimeric form to produce anhydride, and the reaction temperature is much lower than that of pure PMAA.

(Keywords: poly(methacrylic acid); poly(ethylene oxide); polymer complex)

INTRODUCTION

Poly(methacrylic acid) (PMAA) acts as a proton-donating polymer and forms an inter-polymer complex with poly(ethylene oxide) (PEO), which is a proton acceptor[1–4]. Various studies of the complexation mechanism have been carried out using pH[1,2], viscosity[3] and potentiometric measurements[4]. These studies show that PMAA forms a complex with PEO at an equimolar unit ratio, and that the hydrophobic interactions between the CH_2 groups of PEO and the CH_3 groups of PMAA stabilize the complex. As for the miscibility in the solid state, the glass transition temperature (T_g) of the PEO/PMAA complex was examined through torsional braid analysis[5]. A single T_g is observed at 453 K, which is different from those of pure PEO (158–200 K) and PMAA (483 K). This indicates thermodynamic homogeneity of the complex. In solids, the existence of two forms of hydrogen bonding in the complex has been pointed out by i.r. measurements[5,6]. The carboxyl group of PMAA forms hydrogen bonds either with PEO (the complex form) or among PMAA (the dimeric form) (*Figure 1*). It was also shown that the fraction of the complex form is about 70% at 303 K[6]. Further, the i.r. study indicated that, with increasing temperature, the complex form decreases concomitant with an increase of the dimeric form.

High-resolution solid-state ^{13}C n.m.r. has been a powerful method to investigate hydrogen bonding in the solid state. In fact, Maunu *et al.* observed two resolved signals for the carboxyl carbon of PMAA in the complex[7]. In this work, we assigned these peaks to the above-mentioned two forms of hydrogen bonding. We also studied the morphology of the PEO/PMAA complex. We employed the Goldman–Shen[8] pulse sequence combined with cross-polarization/magic-angle spinning (CP/MAS) to estimate the distances between PEO and PMAA. Further, the effects of complexation upon molecular motion were investigated by observing the temperature dependence of the ^{13}C linewidth (T_2) and the ^{1}H spin–spin relaxation time (T_2). Furthermore, we investigated the thermal degradation of PMAA in the PEO/PMAA complex.

EXPERIMENTAL

Samples

PEO with a molecular weight of 20 000 was obtained from Asahidenka Co. PMAA with molecular weight of

* To whom correspondence should be addressed
† Present address: Department of Chemistry, Faculty of Science, Kyoto University, Kyoto 606, Japan

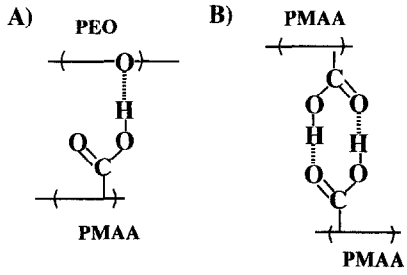

Figure 1 Two forms of hydrogen bonding postulated for the carboxyl of PMAA in the PEO/PMAA complex: (A) hydrogen bonding between PMAA and PEO (a complex form) and (B) hydrogen bonding among PMAA (a dimeric form)

60 000 was purchased from Nippon Junyaku Co. PEO and PMAA were separately dissolved in water (3 wt%), and their pH values were adjusted to 2.0 by adding 1 N HCl solution. The PEO and PMAA solutions were mixed for three different compositions of (a) 2/1, (b) 1/1 and (c) 1/2 in monomer units. In all cases, precipitates were formed as soon as the two solutions were mixed. After leaving for one day, the precipitates were collected, washed and dried for two days under vacuum at 298 K.

The composition of the PEO/PMAA complex was determined by the intensities of the ^{1}H n.m.r. signals of the precipitates, dissolved in dimethylsulfoxide-d_6. Composition ratios of (a) 1.2/1.0, (b) 1.0/1.0 and (c) 1.0/1.0 were found. For our n.m.r. studies, we used sample (b).

N.m.r. experiments

The ^{13}C n.m.r. experiments were carried out with a JEOL GX-270 spectrometer operating at resonance frequencies of 270 MHz for ^{1}H and 67.5 MHz for ^{13}C. High-resolution solid-state ^{13}C n.m.r. spectra were obtained by the combined use of high-power proton decoupling (d.d.) and magic-angle spinning (MAS). The radiofrequency field strength for both ^{1}H and ^{13}C was about 55.6 kHz. The ^{1}H decoupling frequency was chosen to be 3 ppm down-field from tetramethylsilane (TMS). A double-bearing aluminium oxide rotor was used at a spinning frequency of 5.5 kHz. The setting of the magic angle was monitored by the ^{79}Br n.m.r. spectrum of KBr incorporated in the rotor. The ^{13}C chemical shifts were calibrated in ppm relative to TMS by taking the ^{13}C chemical shift of the methine carbon of solid adamantane (29.5 ppm) as an external reference standard. The contact time of cross-polarization (CP) was 500 μs. A shorter CP time of 100 μs was used to observe the spectra of pure PEO, and to measure the rotating-frame spin–lattice relaxation times ($T_{1\rho}$) for all the samples. Variable-temperature measurements were accomplished by using a JEOL MVT temperature controller with an accuracy of 1 K.

In the course of our variable-temperature measurements, we noted that, after heating the samples up to higher temperatures (ca. 375 K), the spectrum at room temperature could not be fully reproduced, even after about two weeks. Since the T_g of the complex is very high (453 K), the structural relaxation should take a very long time. Therefore, each variable-temperature measurement was started after we could confirm that further waiting does not induce any appreciable changes in the spectrum. For example, the spectra in *Figure 4* were measured after leaving the samples for at least 4 h at each designated temperature.

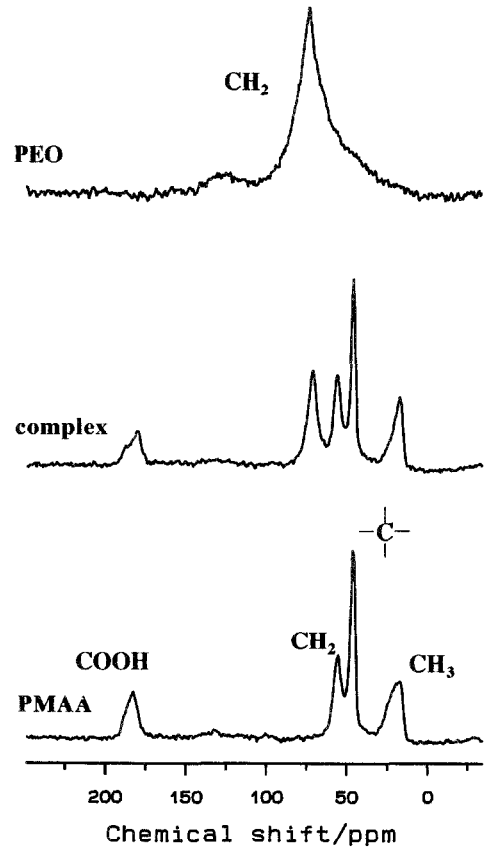

Figure 2 ^{13}C CP/MAS spectra of pure PEO, pure PMAA and the PEO/PMAA complex observed at 307 K. The spectrum of PEO is measured with a short CP times (100 μs)

RESULTS AND DISCUSSION

The ^{13}C CP/MAS spectra of pure PEO, pure PMAA and the PEO/PMAA complex at 307 K are shown in *Figure 2*. Assignments were referenced to the previous reports[9,10]. The effects of complexation are appreciable for the lineshape of the CH_3 carbon of PMAA, the CH_2 carbon of PEO and the carboxyl carbon of PMAA. The change of CH_3 carbon lineshape may be attributed to the hydrophobic interaction with the CH_2 group of PEO in the complex. The latter two lineshapes will be examined closely below.

Two hydrogen-bonding forms of PMAA in the complex

To examine fully the lineshape of the carboxyl carbon of PMAA in the complex, we show the expansion of the carboxyl region in *Figure 3A*. The doublet character is clearly seen. By fitting the observed lineshape to a sum of two Gaussian lineshape functions (*Figure 3B*), we obtained the intensity ratio of the higher-field and the lower-field peaks at 66:34. On the basis of the ratio observed by the i.r. results[6], we assigned the higher-field one to the complex form and the lower-field one to the dimeric form. The chemical-shift value of the peak at higher field is 180 ppm, and that of the lower-field peak is 187 ppm. It is worth noting that the chemical shift of the dimeric form differs from that of pure PMAA (183 ppm), and the linewidth of the former is narrower than that of the latter. These observations show that the hydrogen

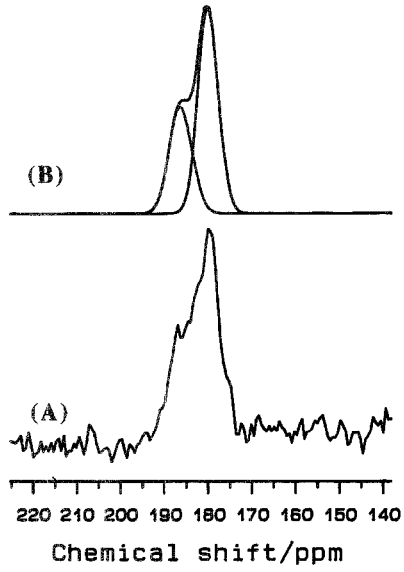

Figure 3 (A) The observed ^{13}C spectrum of the carboxyl carbon of PMAA in the PEO/PMAA complex. (B) The simulated spectrum using two Gaussian lineshapes. The higher-field peak is assigned to the complex form, and the lower-field one is assigned to the dimeric form

bonding among PMAA is stronger and better ordered in the complex than that in pure PMAA. This is consistent with the i.r. results, which show that the hydrogen bonding in pure PMAA is disordered as compared to that in the complex[5].

Figure 4 shows the temperature dependence of the ^{13}C CP/MAS spectra of the carboxyl carbon in the complex. With increasing temperatures, the amount of the lower-field peak (the dimeric form) increases concomitant with the decrease of the higher-field peak (the complex form). This indicates that the inter-polymer hydrogen bonding between PMAA and PEO is destroyed and PMAA is rearranged into the dimeric form. This rearrangement

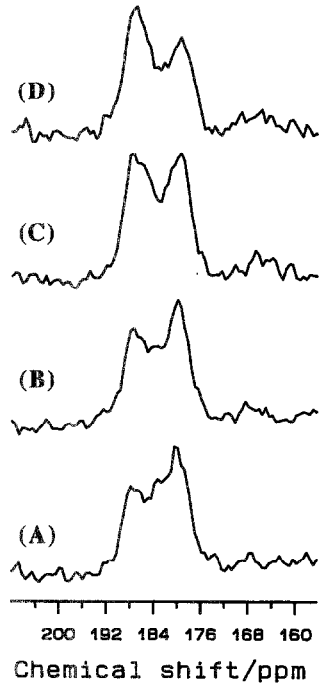

Figure 4 The spectra of the carboxyl region of the PMAA in the PEO/PMAA complex at various temperatures: (A) 315 K, (B) 337 K, (C) 307 K, and (D) 381 K

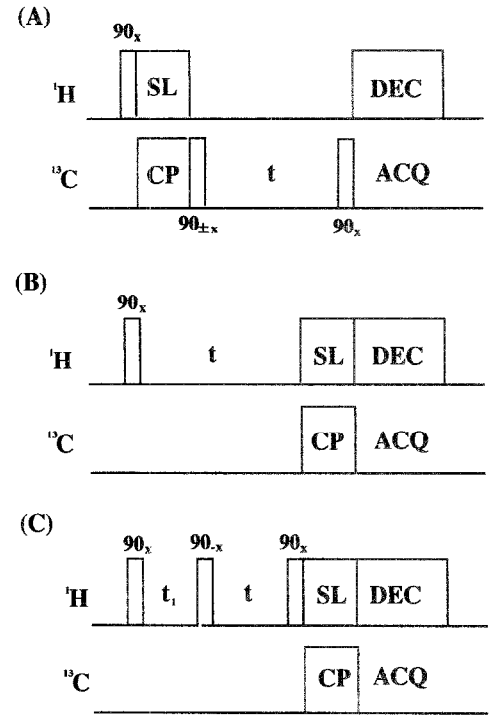

Figure 5 Pulse sequences used in this work: (A) the Torchia sequence for the selective observation of a composition with a long ^{13}C T_1 value; (B) the sequence for the ^1H T_2 measurement; and (C) the Goldman–Shen sequence for the spin-diffusion measurement

was found to be irreversible, showing that the complex form is not the most stable form.

The structure of PEO in the complex

Further examination of *Figure 2* shows that the linewidth of the CH_2 peak of PEO changes on complexation. For pure PEO, the linewidth at half height is about 1000 Hz, while that for the PEO/PMAA complex is about 350 Hz. The line broadening of pure PEO is due to the characteristic molecular motion in the crystalline phase, whose frequency is of the order of the ^1H decoupling frequency[11]. Close examination of the temperature dependence of the ^{13}C linewidth will be discussed below. Here, we attribute the change of linewidth upon complexation to the morphological change of PEO.

Pure PEO is a semicrystalline polymer. At 305 K, the crystalline phase shows a long ^{13}C spin–lattice relaxation time ($T_{1C} = 15$ s), while the amorphous phase shows a T_{1C} value of 0.1 s (ref. 12). By utilizing the different relaxation times between the crystalline and amorphous phases, we can examine whether the crystalline phase exists in the complex. We have employed the Torchia sequence[13] (*Figure 5A*) with a delay time t of 1.5 s to observe the crystalline phase selectively. For pure PEO, the intensity observed with the Torchia sequence (*Figure 6B*) is similar to that observed from the normal CP/MAS spectrum (*Figure 6A*). This shows that a delay time of 1.5 s does not appreciably affect the signal of the crystalline phase. On the other hand, the peak of PEO in the complex disappeared when we applied the Torchia sequence (*Figure 6D*). This indicates that the crystalline phase of PEO is destroyed in the complex. As a reference, we show the spectrum observed by using the conventional CP technique with a contact time of 100 μs (*Figure 6C*).

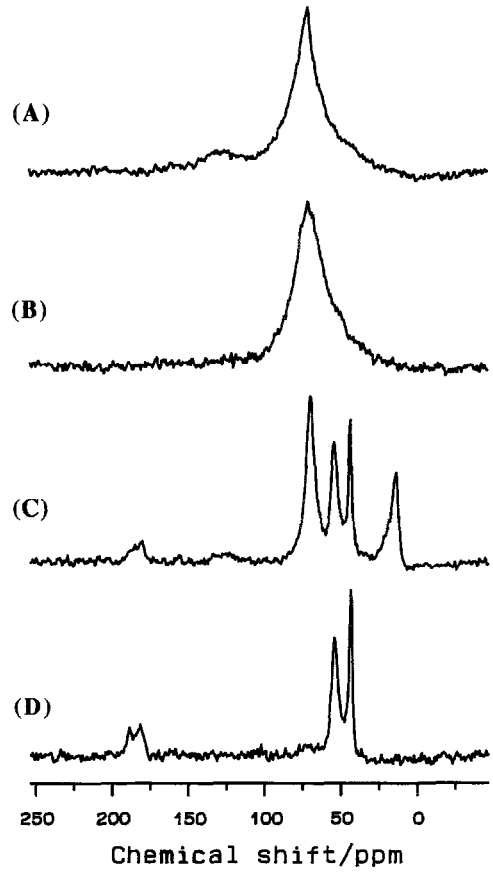

Figure 6 (A) and (B) ^{13}C spectra of pure PEO; (C) and (D) ^{13}C spectra of the PEO/PMAA complex. (A) and (C) were observed by using the conventional CP sequence with the contact time of 100 μs. (B) and (D) were observed by using the Torchia sequence depicted in *Figure 5A*

The reduced linewidth is responsible for the amorphous structure of PEO. A similar reduction of the ^{13}C linewidth of PEO upon blending has also been observed for the PEO/poly(vinyl phenol) (PVPh) blends[14].

Spin–spin relaxation measurements

We examined the ^1H spin–spin relaxation times (T_2) of the complex at 307 and 375 K by using the pulse sequence shown in *Figure 5B*. The observed T_2 values are summarized in *Table 1*. At both temperatures, the observed ^1H T_2 decay of PMAA could be explained as a single Gaussian decay. This indicates that the two kinds of PMAA (the complex form and the dimeric form) cannot be distinguished by their ^1H T_2.

Figure 7 shows the ^1H T_2 decay curve of PEO in the complex at 375 K. The observed decay was fitted to the sum of a Gaussian decay function and a Lorentzian function. The Gaussian component of $^1HT_2$ represents the rigid part of PEO and the Lorentzian one represents the mobile one. At least two PEO segments with different motional states exist in the complex. As shown above, PEO forms an amorphous phase in the complex. Hence, these two PEO segments cannot be attributed to the amorphous and crystalline phases of PEO, and we relate them to the two different hydrogen-bonding forms in the complex. We attribute the rigid Gaussian component to PEO forming hydrogen bonding with PMAA, and the mobile Lorentzian component to PEO that does not form hydrogen bonding. Hereafter, we denote the former PEO as the rigid PEO, and the latter as the mobile PEO.

Table 1 The ^1H spin–spin relaxation times (T_2) of the PEO/PMAA complex at 370 K and 375 K[a]

	PMAA (μs)			PEO (μs)[b]
	CH_2	CH_3	COOH	CH_2
307 K	19 ± 3	26 ± 4	32 ± 4	17 ± 1 (G) (51%) 33 ± 9 (L)
375 K	21 ± 1	31 ± 2	27 ± 3	36 ± 1 (G) (23%) 186 ± 20 (L)

[a] Errors are 2.5σ
[b] G and L denote the Gaussian and the Lorentzian component, respectively

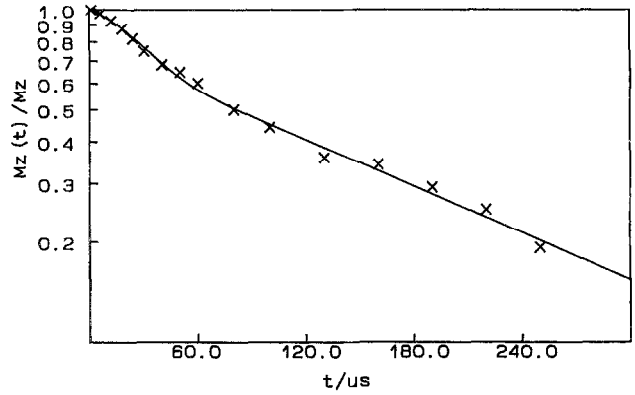

Figure 7 The normalized ^1H T_2 decay curve of PEO in the PEO/PMAA complex at 375 K. The full curve represents the superposition of a fast Gaussian with $T_2 = 36\,\mu s$ and a slow Lorentzian with $T_2 = 186\,\mu s$

The morphology of the PEO/PMAA complex

In this section, we investigate the morphology of the PEO/PMAA complex using the modified Goldman–Shen pulse sequence (*Figure 5C*)[8,14–17]. At 375 K, ^1H T_2 of the mobile PEO (186 μs) is much longer than those of the other protons (< 36 μs) (*Table 1*). Therefore, a T_2 decay time of 50 μs after the first 90° pulse for ^1H eliminates all ^1H transverse magnetizations except that of the mobile PEO. The remaining transverse magnetization of the mobile PEO is transferred to the longitudinal one by the second 90° pulse. During a diffusion period, the ^1H spin energy is transported via the spin-diffusion mechanism from the mobile PEO to the rigid PEO and PMAA. After a certain mixing time t_m the resulting ^1H magnetizations are transferred to the ^{13}C spins through the CP technique. In this way, we can examine the spin diffusion from the mobile PEO to the rigid PEO and PMAA by monitoring the intensities of the ^{13}C signals at various mixing times. We have attributed the rigid PEO to those segments which form hydrogen bonding with PMAA, and the mobile PEO to those segments in which such bonding is absent. The distance between the mobile PEO and PMAA should be longer than that between the rigid PEO and PMAA. Therefore, the spin diffusion between the mobile PEO and PMAA would show the maximum distance between PEO and PMAA.

Figure 8 shows the ^{13}C spectra for various mixing times. The top spectrum has the shortest mixing time and shows only the signal from the mobile PEO. With increasing mixing time, the intensity of the PEO peak decreases and those of the PMAA peaks increase. This shows that spin diffusion occurs between the mobile PEO

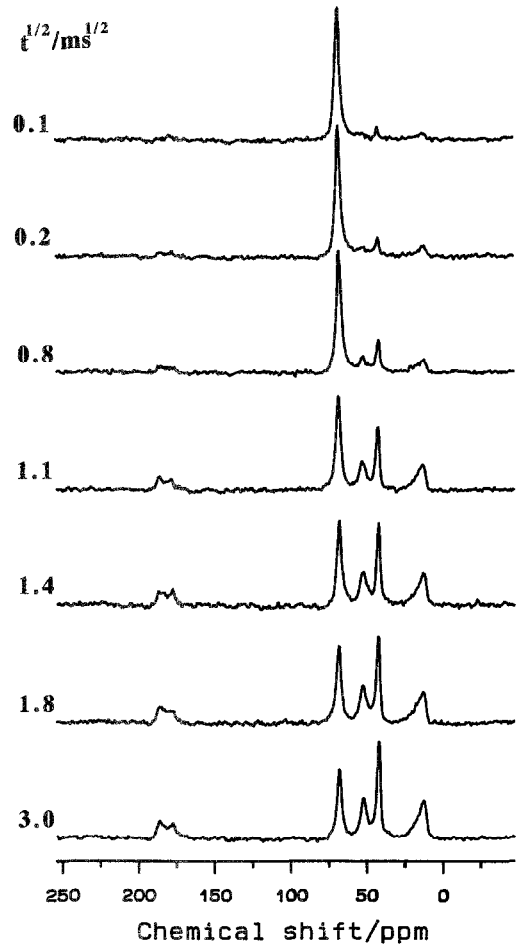

Figure 8 The ^{13}C CP/MAS spectra observed by the modified Goldman–Shen pulse sequence (*Figure 5C*) with a fixed delay time t_1 of 50 μs at 375 K. At the left side of the spectra, the square root of the diffusion time $t^{1/2}$ is shown

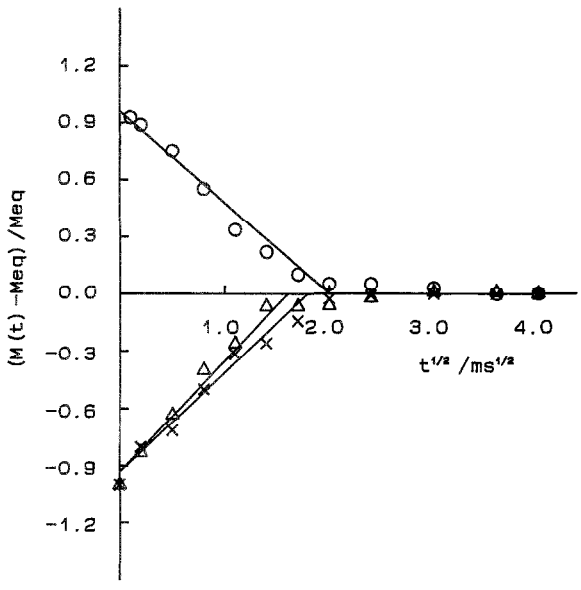

Figure 9 Plot of the relative ^{13}C magnetization vs. the square root of the spin-diffusion time $t^{1/2}$: (○) the observed data through the CH_2 resonance of PEO, (△) the higher- and (×) the lower-field resonance of carboxyl carbon of PMAA

and PMAA. It is interesting to note that the rate of recovery of the carboxyl magnetization for the dimeric form is almost identical to that for the complex form. This indicates that the distances between the mobile PEO and PMAA are similar in the complex form and in the dimeric form. In the current experiment, it is difficult to examine the spin diffusion process between the mobile PEO and the rigid PEO, because the signals from the two PEO segments overlap. Therefore, we treat the observed results as a simple spin-diffusion process between the two ^1H groups of PEO and PMAA.

Figure 9 shows the mixing-time dependence of the relative intensity of the $^{13}CH_2$ signal of PEO, as well as those of the two carboxyl resonances of PMAA. By assuming diffusion in one dimension, one can write the mean-square spin-diffusion path length $\langle l^2 \rangle$ during a mixing time t as[14,15]:

$$\langle l^2 \rangle = \tfrac{4}{3} Dt \tag{1}$$

The diffusion constant D may be given as[16]:

$$D = \frac{2r_0^2}{T_2} \tag{2}$$

where r_0 is the van der Waals radius of a hydrogen atom (1.17 Å) and T_2 is the ^1H T_2 of the mobile PEO. Spiegel *et al.* showed that these simple equations are applicable to estimate the domain size of a system containing both rigid and mobile components, provided that the ^1H T_2 relaxation time for the mobile polymer is less than 1 ms[18].

From equations (1) and (2), and ^1H T_2 of the mobile PEO (186 μs), we deduced a lower limit of the effective path length between the mobile PEO and PMAA in the complex to be 7 Å and in the dimeric form to be 8 Å. This indicates that PEO and PMAA are miscible on a molecular scale, and the dimeric and complex forms of PMAA should appear within a few segments in one PMAA chain. The distance between the rigid PEO and PMAA in the complex form should be even closer than that between the mobile PEO and PMAA in the complex. Therefore, the estimated short distance (7 Å) between the mobile PEO and PMAA suggests that both the rigid and the mobile PEO appear within a few segments in one PEO chain.

Spin–lattice relaxation experiment

In this section, we examine the ^1H spin–lattice relaxation time in the laboratory frame (T_1) and that in the rotating frame ($T_{1\rho}$). The ^1H T_1 and $T_{1\rho}$ measurements provide simple approaches to investigate miscibility; if the domain size is smaller than the maximum spin-diffusion path length $\langle l^2 \rangle$ for the particular relaxation experiment, one would observe the same relaxation times for component polymers. The identical ^1H T_1 and ^1H $T_{1\rho}$ values show the miscibility on a few 100 Å scale and a few 10 Å scale, respectively. For the PEO/PMAA complex, Maunu *et al.* have measured ^1H T_1 and $T_{1\rho}$. However, they did not draw a conclusion about miscibility[7].

We examined ^1H T_1 at 307 K and ^1H $T_{1\rho}$ at 307 and 237 K. The observed relaxation times are listed in *Table 2*. For pure PEO, at 307 K, two ^1H $T_{1\rho}$ were observed, which have been attributed to the crystalline and amorphous phases[14,19]. At 237 K, the $T_{1\rho}$ values for the two phases become too close to discriminate.

For the PEO/PMAA complex, the observed ^1H T_1 value of PEO is almost the same as that of PMAA. This result for the miscibility of the complex is consistent with the outcome of the Goldman–Shen experiment. However,

Table 2 The ^1H spin–lattice relaxation time in the laboratory frame (T_1) and in the rotating frame ($T_{1\rho}$) at 307 K and 237 K[a,b]

	T_1 (s) (307 K)	$T_{1\rho}$ (ms) (307 K)	$T_{1\rho}$ (ms) (237 K)
Pure			
PEO	3.65 ± 0.19	0.20 ± 0.03	20.70 ± 1.61
PMAA	0.44 ± 0.03	4.60 ± 0.20	2.21 ± 0.30
Complex			
PEO	0.50 ± 0.06	0.71[b]	2.10 ± 0.21
PMAA	0.52 ± 0.02	5.00[b]	2.21 ± 0.30

[a] Errors are 2.5σ
[b] The $T_{1\rho}$ value is obtained by using equation (3)

the observed ^1H $T_{1\rho}$ decay curve of PEO differs significantly from that of PMAA (*Figure 10*). These different $T_{1\rho}$ curves may be interpreted as immiscibility of the PEO/PMAA complex on a scale of a few 10 Å. This would be inconsistent with the result of the Goldman–Shen experiment. Two reasons may be invoked to explain the observed $T_{1\rho}$ relaxation curves for component polymers. One is heterogeneity and the other is motional effects. Below we show that the latter should be responsible in the present case.

In order to analyse the observed decay curves, we treat the spin system as two dipolar-coupled spins A (PEO) and B (PMAA). The equations describing the dynamics of the magnetizations are given as[20]:

$$-\frac{dM_A}{dt} = (K_A + f_B K_c)M_A - f_A K_c M_B \qquad (3a)$$

$$-\frac{dM_B}{dt} = (K_B + f_A K_c)M_B - f_B K_c M_A \qquad (3b)$$

where M_i, f_i and K_i (i = A and B) denote the magnetization, the ^1H mole fraction and the intrinsic relaxation rate of the i spin ($K_i^{-1} = T_{1\rho}$), respectively. K_c is the cross-relaxation (spin-diffusion) rate.

The full curves in *Figure 10* show the calculated results with $K_A = 1.6 \times 10^3\ s^{-1}$ ($T_{1\rho} = 0.71$ ms), $K_B = 0.2 \times 10^3\ s^{-1}$ ($T_{1\rho} = 5.00$ ms) and $K_c = 1.4 \times 10^3\ s^{-1}$. The $T_{1\rho}$ value (0.71 ms) for PEO in the complex is close to the experimental ^1H $T_{1\rho}$ minimum value of pure PEO in the amorphous phase (0.5 ms)[19]. Therefore, the motional frequency of PEO in the complex is close to the strength of the spin-locking field (55.6 kHz). This motion averages the ^1H–^1H dipolar interactions between PEO and PMAA to some extent, and the cross-relaxation rate (K_c) becomes too slow to average K_A and K_B. Thus, incomplete spin diffusion in the PEO/PMAA complex is suggested to be due not to heterogeneity but to motional effects. To confirm this, we performed the $T_{1\rho}$ experiment at 237 K to reduce the motional effects. We observed a single exponential decay for both PEO and PMAA in the complex, and their $T_{1\rho}$ values are almost identical (*Table 2*). A similar observation has been found in polystyrene/poly(vinyl methyl ether) (PS/PVME) blends[21,22].

Here, we would like to summarize the results about the structure of the complex. Two conformations for PMAA in the PEO/PMAA complex are invoked. One is the complex form, in which the carboxyl carbon forms hydrogen bonding with PEO. The carboxyl carbon shows an up-field shift as compared to that in pure PMAA. The ^1H T_2 measurements show that the motion of the hydrogen-bonded PEO is restricted. The other conformation for PMAA is the dimeric form, in which no hydrogen bonding exists between PEO and PMAA. The carboxyl carbon in the dimeric form shows a down-field shift. The ^1H T_2 measurements show that no hydrogen-bonded PEO is mobile. The spin-diffusion study shows that the two conformations of PMAA and the two motionally different forms of PEO coexist locally, and the PEO/PMAA complex is homogeneous on a segmental scale.

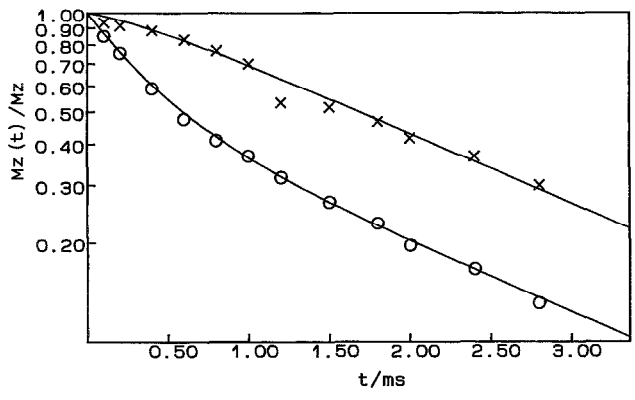

Figure 10 The normalized ^1H $T_{1\rho}$ curve for PMAA (×) and PEO (○) in the complex. The full curves are calculated using equation (3) with parameters $K_A = 1.6 \times 10^3\ s^{-1}$, $K_B = 0.2 \times 10^3\ s^{-1}$ and $K_c = 1.4 \times 10^3\ s^{-1}$

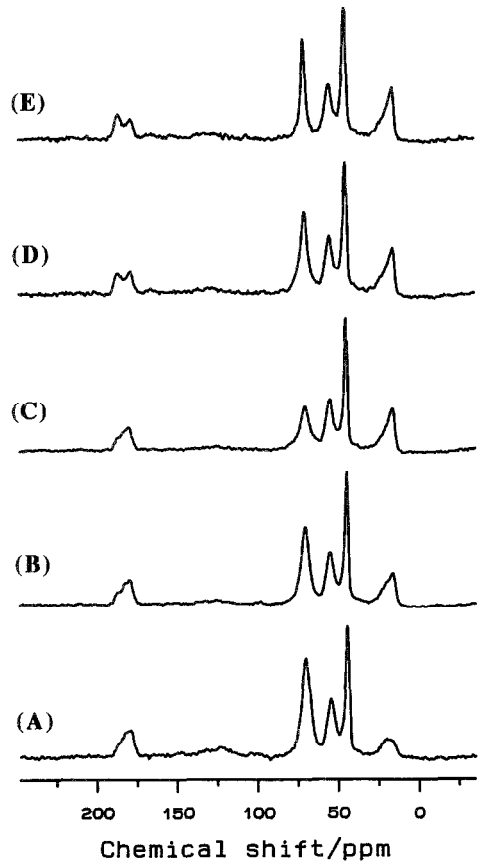

Figure 11 ^{13}C CP/MAS n.m.r. spectra of the PEO/PMAA complex at various temperatures: (A) 230 K, (B) 260 K, (C) 307 K, (D) 348 K, and (E) 381 K

Effects of complexation on molecular motion

From the ^1H T_2 and $T_{1\rho}$ measurements, we have shown that PEO is much more mobile than PMAA. In this section, the chain dynamics of PEO in the PEO/PMAA complex below T_g is discussed by analysing the ^{13}C linewidth. *Figure 11* shows the ^{13}C CP/MAS spectra of the complex at various temperatures. Within our temperature range (210–381 K), the linewidths of the PMAA peaks are almost temperature-independent. On the other hand, the linewidth of PEO shows broadening with increasing temperature from 210 to 307 K, where the maximum broadening is reached. A further temperature increase brings about line narrowing.

As shown by the analysis of the $T_{1\rho}$ decay curves, the $T_{1\rho}$ value of the PEO in the complex at 307 K is close to the $T_{1\rho}$ minimum value of pure amorphous PEO[19]. The characteristic motional frequency at 307 K should be close to the strength of the ^1H r.f. field (55.6 kHz). Since molecular motion with a frequency close to the intensity of the ^1H decoupling field interferes with the ^1H decoupling, it leads to a broadening of the ^{13}C linewidth[23,24]. The observed maximum broadening of the ^{13}C linewidth at 370 K should be attributed to the motion related to the $T_{1\rho}$ minimum.

The observed temperature dependence of the ^{13}C linewidth of the polymer under high-power ^1H decoupling may be expressed by the following empirical equation[25]:

$$\delta = \delta_0 + \delta_1(2/\pi)\arctan[\alpha(T_0 - T)] + \lambda M_2 J(\omega_1, \tau) \quad (4)$$

The first term represents the intrinsic linewidth arising from various static line broadenings. The second term describes the motional narrowing of the distribution (δ_1) of the isotropic chemical shift. The arctangent dependence was assumed and α describes the steepness of the narrowing. T_0 is the characteristic temperature designating the onset of the molecular motion. The third term represents the linewidth arising from the ^{13}C–^1H dipole interaction[23,24]. M_2 represents the powder average of the second moment of the ^{13}C–^1H dipolar interaction; and λ is a reduction factor of the second moment ($0 < \lambda < 1$); for isotropic motion $\lambda = 1$. The factor λ decreases as the motion becomes more anisotropic. $J(\omega_1, \tau)$ is the spectral density function of the motion of the ^{13}C–^1H internuclear vector with a correlation time τ and a decoupling frequency ω_1:

$$J(\omega_1, \tau) = \frac{\tau}{1 + \omega_1^2 \tau^2} \quad (5)$$

The maximum line broadening is achieved when the motional frequency is equal to the ^1H decoupling frequency ($\omega_1 \tau = 1$). We assume that the correlation time has an Arrhenius-type dependence on the temperature:

$$\tau = \tau_0 \exp\left(\frac{E_a}{RT}\right) \quad (6)$$

where E_a is the activation energy and τ_0 is the correlation time at infinite temperature. We fitted the linewidth of PEO to equations (4)–(6), and the best-fit parameters are $E_a = 6.7$ kcal mol^{-1}, $\lambda = 0.079$, $\tau_0 = 4.8 \times 10^{-11}$ s, $T_0 = 270.4$ K, $\delta_0 = 213.0$ Hz, $\delta_1 = 138.3$ Hz and $\alpha = 0.069$.

The observed activation energy ($E_a = 6.7$ kcal mol^{-1}) and the reduction factor ($\lambda = 0.079$) are smaller than those of PEO in the PEO/PVPh blends ($E_a \sim 10$ kcal mol^{-1}, $\lambda \sim 0.13$)[11]. This may be understood as follows: in both the PEO/PMAA complex and the PEO/PVPh blends, the motional freedom of PEO is restricted by the interpolymer hydrogen bonding with the counterpart polymer. If we consider T_g of a polymer as a measure of its mobility, PMAA ($T_g = 483$ K) is less mobile than PVPh ($T_g = 393$ K). The hard PMAA allows only a small-amplitude motion of PEO, leading to smaller values of E_a and λ (less isotropic).

Thermal degradation

We further examined the structural change of the complex at much higher temperatures (305–523 K). The complex was heated up to a certain temperature for 1 h. After heating, the sample was cooled by immersing into ice–water to freeze the structure. *Figure 12* shows the ^{13}C CP/MAS spectra of PEO/PMAA treated at different temperatures. The two carboxyl peaks can be appreciable for the samples with heat-treatment temperatures below 383 K. The characteristic lineshape change is similar to that in *Figure 4*, and was already explained in the previous section. The sample heated at 423 K exhibits a new peak at 173 ppm. On the basis of the previous reports[26,27], we assigned this peak to the anhydride due to dehydration of PMAA. For pure

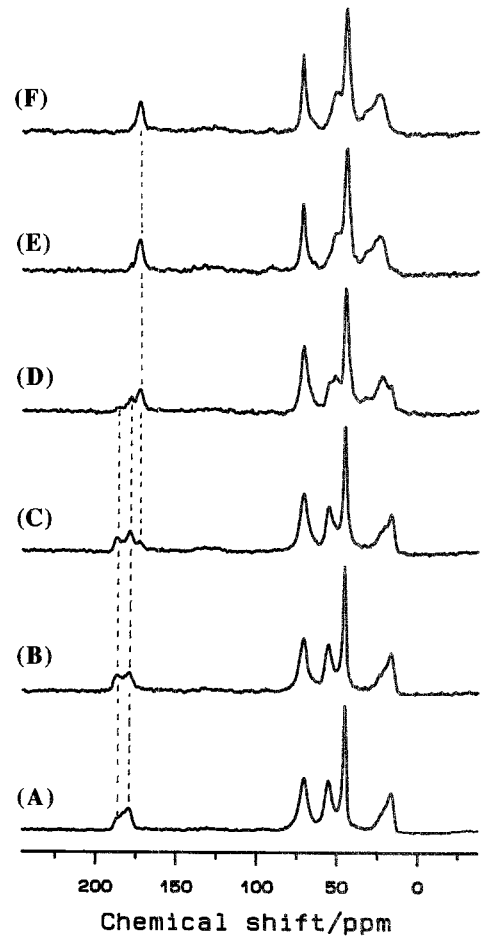

Figure 12 ^{13}C CP/MAS spectra of the PEO/PMAA complex at room temperature, after heat treatment for 1 h: (A) without heating; (B) heated at 383 K; (C) heated at 423 K; (D) heated at 453 K; (E) heated at 483 K; and (F) heated at 523 K

Table 3 The relative population of the three PMAA structures after various heat treatments

Heat treatment temperature (K)	Complex form (%)	Dimeric form (%)	Anhydride form (%)
no heating	66	34	–
383	50	50	–
423	50	34	16
453	30	8	62
483	–	–	100
523	–	–	100

PMAA, dehydration occurs above 483 K[28]. Therefore, for the complex, dehydration occurs at much lower temperature than for pure PMAA. A similar reduction of the dehydration temperature has been reported for the poly(vinyl alcohol)/poly(methacrylic acid) (PVA/PMAA) complex[27].

We fitted the carboxyl lineshape in *Figure 12* to a sum of three Gaussian lineshapes, and the relative intensities deduced for the three peaks are collected in *Table 3*. At 423 K, the ratio of the complex form is similar to that at 383 K, while the ratio of the dimeric form decreases from 50% to 34% concomitant with an increase of the anhydride peak. This result causes us to conclude that the dehydration reaction occurs in the dimeric form. It is worth noting that the dehydration reaction becomes appreciable around T_g of the complex (453 K). A similar relation between the dehydration temperature and T_g was observed for pure PMAA[26] and the PVA/PMAA complex[27].

To conclude, PEO is much more mobile than PMAA. Therefore, the motion of PEO is responsible for breaking the complex form with increasing temperature. The released PMAA is rearranged to the dimeric form, and further heat treatment at temperatures near T_g induces dehydration of PMAA in the dimeric form.

REFERENCES

1 Osada, J. Y. *Polym. Sci., Polym. Chem. Edn.* 1979, **17**, 3485
2 Osada, Y., Papisov, I. M., Kabanov, V. A. and Kargin, V. A. *Doklady Acad. Nauk. USSR.* 1970, **191**, 399
3 Bailey, F. E., Lundberg, R. D. Jr. and Callard, R. W. *J. Polym. Sci. (A)* 1964, **2**, 845
4 Antipina, A. D., Baranovskii, V. Yu., Papisov, I. M. and Kabanov, V. A. *Vysokomol. Soedin. (A)* 1972, **14**, 941
5 Kim, H. J. and Tonami, H. *Kobunshi Ronbunshu* 1978, **35**, 395
6 Kim, H. J., Mogami, K., Sakamoto, M. and Tonami, H. *Kobunshi Ronbunshu* 1983, **40**, 637
7 Maunu, S. L., Kinnunen, J., Sojiamo, K. and Sundholm, F. *Polymer* 1993, **34**, 1141
8 Goldman, M. and Shen, L. *Phys. Rev.* 1966, **144**, 321
9 Zhang, X., Takegoshi, K. and Hikichi, K. *Polym. J.* 1991, **23**, 79
10 Schaefer, J. *Macromolecules* 1971, **4**, 98
11 Zhang, X., Takegoshi, K. and Hikichi, K. *Macromolecules* 1993, **26**, 2198
12 Decther, J. J. *J. Polym. Sci., Polym. Lett. Edn.* 1985, **23**, 261
13 Torchia, D. A. *J. Magn. Reson.* 1978, **30**, 613
14 Zhang, X., Takegoshi, K. and Hikichi, K. *Macromolecules* 1992, **25**, 2336
15 Zhang, X., Takegoshi, K. and Hikichi, K. *Polym. J.* 1992, **24**, 1403
16 Assink, R. A. *Macromolecules* 1978, **11**, 1233
17 VanderHart, D. L. *Makromol. Chem., Macromol. Symp.* 1990, **34**, 125
18 Spiegel, S., Schmidt-Rohr, K., Boeffel, C. and Spiess, H. W. *Polymer* 1993, **34**, 4566
19 Johansson, A. and Tegenfeldt, J. *Macromolecules* 1992, **25**, 4718
20 Stejskal, E. O., Schaefer, J., Sefcik, M. D. and McKay, R. A. *Macromolecules* 1981, **14**, 275
21 Chu, C. W., Dickinson, L. C. and Chien, J. C. W. *J. Appl. Polym. Sci.* 1990, **41**, 2311
22 Asano, A., Takegoshi, K. and Hikichi, K. *Polymer* 1994, **35**, 5630
23 VanderHart, D. L., Earl, W. P. and Garroway, A. N. *J. Magn. Reson.* 1981, **44**, 361
24 Rothwell, W. P. and Waugh, J. S. *J. Chem. Phys.* 1981, **74**, 2721
25 Takegoshi, K. and Hikichi, K. *J. Chem. Phys.* 1991, **94**, 3200
26 Fyfe, C. A. and McKinnon, M. S. *Macromolecules* 1986, **19**, 1909
27 Zhang, X., Takegoshi, K. and Hikichi, K. *Polymer* 1992, **33**, 718
28 McGaugh, M. C. and Kottle, S. *J. Polym. Sci. (A-1)* 1968, **6**, 1243